〈ノート〉

Physical and Observer Performance on the Image Quality with Scintillation Camera

Hiroyuki SHINOHARA* and Yasushi KOGA*

Introduction

Spatial resolution characteristics of imaging system have been measured by objective physical performance such as FWHM or MTF, or subjectively in terms of organ or bar phantom. These common method have the advantage of being simple to perform. However the method does not always approximate the clinical problem (namely, the detection of a focal lesion within an activity distribution).[1)]

Rollo and Schulz developed the concept of contrast efficiency which was defined to quantitatively measure how well an imaging system will detect a spherical void of activity within an activity distribution.[1)] On the basis of their theory, Rollo proposed Rollo (overall performance) phantom.[2)] The phantom was designed so that images obtained with a given system could be subjectively or quantitatively evaluated.

We made a modified Rollo phantom and used for visual evaluation of ^{99m}Tc scintiphotos, made with the same scintillation camera but with different collimators. The obtained results were discussed with the difference of spatial resolution for three collimator systems measured by physical performance. The advantage and disadvantage of modified Rollo phantom was discussed.

Materials and Methods

Fig. 1 shows drawing of the modified Rollo phantom. It consists of sixteen spherical cold lesions having four different size and object contrast. In the original Rollo phantom, sixteen spherical lesions are situated at equal distances from the upper and lower surfaces, so it is symmetric with respect to the axis connecting the spherical lesions having the same radius. These are not similarly situated in the modified phantom, in order to include different scattering effects depending on which surface faces toward the detector. Thus in the modified phantom the distance between a spherical lesion and detector varies along with the object contrast as is shown in Fig. 1. As the spatial resolution of parallel hole collimator degrades with increasing collimator-source distance, it is necessary to make corrections to examine the collimator's lesion-detecting ability as a function of object contrast. However we are not concerned with the absolute lesion-detecting ability of the collimator but relative one, the modified phantom is still be useful in the present work.

^{99m}Tc images were made with a 20% energy window, using Searle LFOV high resolution parallel hole, 360-keV, and medium (300-keV) collimators, here coded "HRP", "360 keV", and "300 keV", respectively. The system spatial resolution expressed as FWHM for ^{99m}Tc source is shown in Fig. 2.[3)] On the basis of the FWHM, the spatial resolution characteristics of the three collimators were evaluated by contrast efficiency (Ec) defined by Eq. 1.[1)]

$$Ec = \frac{\text{Image contrast } (C_I)}{\text{Object contrast } (C_O)} = \frac{\int_0^{\alpha} fL(f)\,MTF(f)\,df}{\int_0^{\alpha} fL(f)\,df} \quad (1)$$

*Department of Radiology, Fujigaoka Hospital, Showa University, 1-30, Fujigaoka, Midori-ku, Yokohama-shi, 227 Japan
受付：55年9月2日
最終稿受付：55年11月27日
別刷請求先：横浜市緑区藤が丘 1-30 (〒227)
昭和大学藤が丘病院放射線科
篠 原 広 行

Key words: Physical performance, Observer performance, Modified Rollo phantom

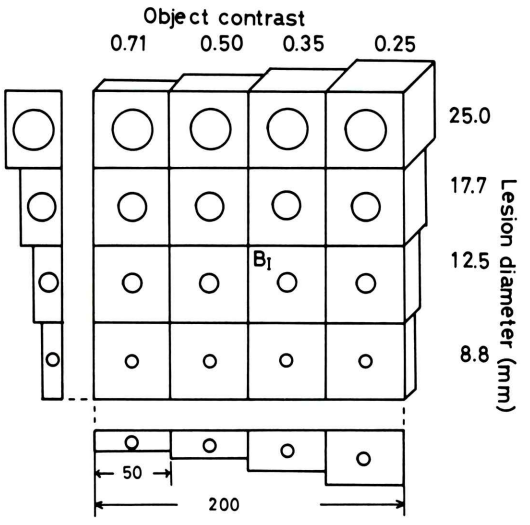

Fig. 1 Design of modified Rollo phantom. Profile of the side view shows how height of each sphere is varied in order to provide each sphere with an object contrast. B_I in the figure denotes the position used for determining the background count density in Figs. 6 and 8–10.

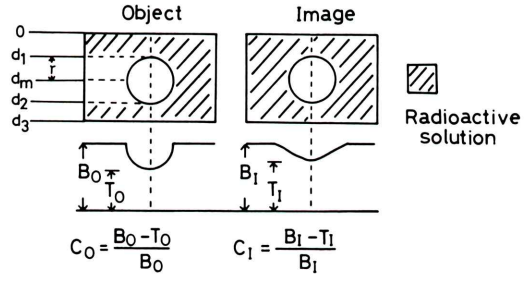

Fig. 3 Pictorial representation of the contrast efficiency concept developed by Rollo et al.[1] Parameters d_1 and d_m are the distances from the surface of phantom to the surface of the spherical lesion and to the center of the sphere, respectively.

where f is the spatial frequency and MTF(f) the modulation transfer function. MTF(f) is calculated assuming line spread function of the imaging system could be approximated to Gaussian function. In this case MTF(f) is calculated as follows:

$$\mathrm{MTF(f)} = \exp(-3.559\,d^2f^2) \qquad (2)$$

d: FWHM

f: spatial frequency (cycles/cm)

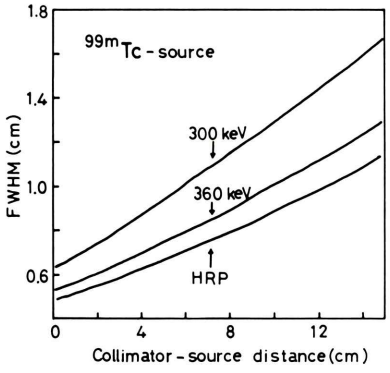

Fig. 2 System spatial resolution expressed as FWHM for Searle LFOV three collimator systems (for ^{99m}Tc source).[2]

L(f) is the transfer function for any spherical lesion having radius r, and is found as follows:

$$\mathrm{L(f)} = \frac{3\sin(2\pi fr)}{(2\pi fr)^3} - \frac{3\cos(2\pi fr)}{(2\pi fr)^2} \qquad (3)$$

The contrast efficiency concept is outlined in Fig. 3, which shows an object that contains a spherical cold lesion within an activity distribution. If this object were to be scanned with an imaging system having finite spatial resolution-i.e., a MTF not equal to unity for all spatial frequencies—the scan profile shown in right hand of Fig. 3 would result. Thus the contrast efficiency measures how well an imaging system will detect a spherical lesion within an activity distribution. The object contrast of Eq. 1 and Fig. 1 is defined by the maximum signal to background ratio corresponding to the center of the spherical lesion, and is given by Eq. 4.

$$C_0 = \frac{B_0 - T_0}{B_0} = \frac{\int_{d_1}^{d_2} \exp(-\mu x)\,dx}{\int_0^{d_3} \exp(-\mu x)\,dx} \approx \frac{2r\exp(-\mu d_m)}{\frac{1}{\mu}(1-\exp(-\mu d_3))} \qquad (4)$$

Since $\mu r \ll 1$ the approximation in the numerator is obtained by series expansions of the exponential functions. The attenuation coefficient μ is 0.15 cm^{-1} for ^{99m}Tc in water[4] and other notaions used in Eq. 4 are shown in Fig. 3.

The lesion-detecting ability of three collimators is compared by imaging the modified Rollo phantom with equal count densities. As collimator performance is dependent on both spatial resolution and plane sensitivity, it is more valid to compare their lesion-detecting ability by imaging the phantom with equal accumulation times. The purpose of this study, however, is to examine the spatial resolution characteristics of three collimators from physical and observer performances points of view, therefore the images obtained with the equal count densities were compared. If the modified Rollo phantom was proved to be useful, the experiments considering system spatial resolution and plane sensitivity would be continued.

The cell background activity surrounding the spherical cold lesions in the original and modified Rollo phantoms is varied so as to give the different object contrast to the lesion with the same diameter. Practically this is done by varing the height of radioactive solution filled in the each cell. Therefore recorded count density for sixteen background cells is different each other. We defined the count density as the number of counts which was recorded in the cell background area of 1 cm^2 surrounding the lesion with diameter 12.5 mm having object contrast 0.35 (B_I in Fig. 1).

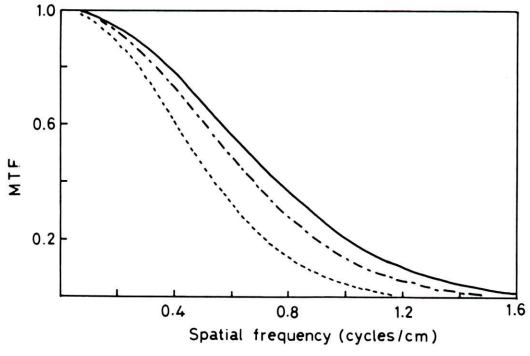

Fig. 4 System spatial resolution expressed as MTF at collimator-source distance of 5 cm. When the phantom is imaged at the surface of collimator, the maximum distance between the surface of collimator and center of spherical lesion is 5 cm, then MTF is derived from the FWHM at collimator-source distance of 5 cm in Fig. 2. ——: HRP, – – –: 360 keV; ……: 300 keV collimator.

Consequently, background count density for the lesion with diameter 25.0 mm having object contrast 0.25 is relatively higher than standard count density B_I, while background count density for the lesion with diameter 8.8 mm having object contrast 0.71 is relatively lower than the B_I. The visibility of photon-deficient lesions changes according to which cell in Fig. 1 is selected as a standard for expressing the background count density. Ideally it should be selected so that the sixteen photon-deficient lesions could be seen if the phantom was imaged with the high resolution collimator system. After several experiments, we chose the cell above-mentioned as a standard. With regard to this point it will be discussed in later paragraph.

The modified Rollo phantom was imaged with the count densities of 0.5, 1.5, and 2.5 kcounts/cm^2 at different collimator-source distances: (1) surface of the collimator, and (2) apart 10 cm from the collimator. The phantom images were studied by four observers to determine how well photon-deficient lesions could be seen. The observers were one physicist and three technologists with two or more years of experience in nuclear midicine. The observers indicated their level of confidence according to the following scale: 4=confidence approaching 100% that a lesion is present; 3=less confidence (~75%) that a lesion is present; 2=~50% confidence; and 1=lesion is scarecely present, confidence

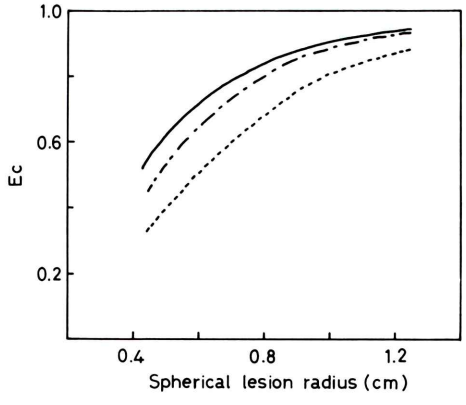

Fig. 5 System spatial resolution expressed as Ec at collimator-source distance of 5 cm. See the notes in Fig. 4.

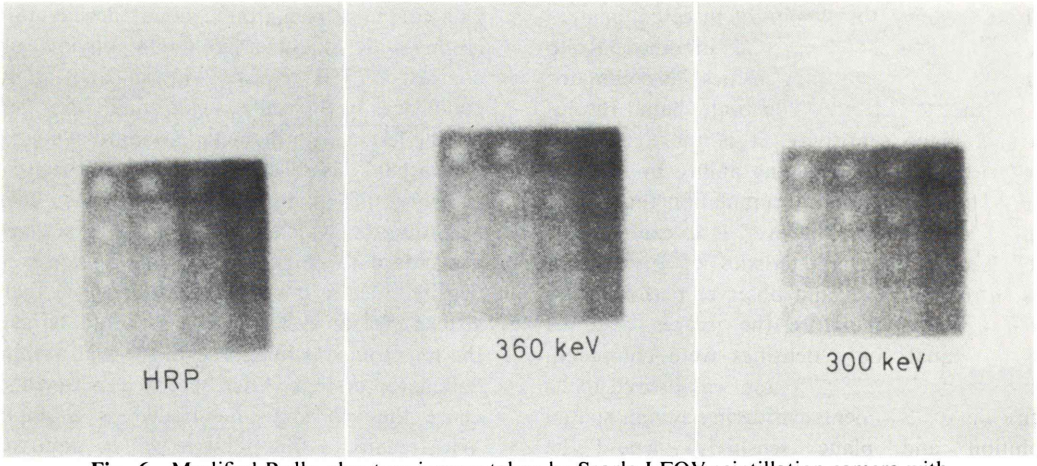

Fig. 6 Modified Rollo phantom images taken by Searle LFOV scintillation camera with the count density of 2.5 kcounts/cm^2. With regard to the arrangement of spherical cold lesions, see Fig. 1.

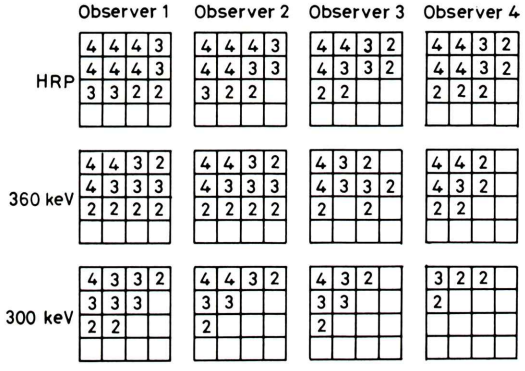

Fig. 7 Detection tests performed by four observers on the modified Rollo phantom images in Fig. 6. Numbers 4, 3, and 2 denote the level of confidence 100, 75, and 50%, respectively while blank corresponds to level of confidence 0% (number 1 is not written but abbreviated).

minimum (~0%). The detection tests were repeated three times and the average value of level of confidence was calculated.

Results

Fig. 4 and 5 show MTF and contrast efficiency, Ec, for three collimator systems, respectively. Ec was calculated for spherical lesion radius between 0.44 cm (minimum lesion radius in the modified Rollo phantom in Fig. 1) and 1.25 cm (maximum lesion radius in Fig. 1). Large spherical lesion corresponds to low frequencies, whereas small spherical lesion corresponds to high frequencies, therefore Ec approaches 1 with an increase in lesion radius as is expected from Eq. 1. As spatial resolution given by MTF is represented in the spatial frequency domain it does not directly answer how well imaging system reconstructs object radioactive distribution in the image plane. On the other hand, as Ec describes spatial resolution in the spatial domain it gives collimator's difference more vividly in the detection of lesions within an activity distribution as is shown in Fig. 5. Namely it shows that the contrast efficiency compares imaging systems on the basis of how their respective MTFs modify the transfer function of spherical lesions of various sizes. It can be seen for example that for spherical lesion with radius 0.8 cm, the output image contrast is 84% of the input object contrast, if the HRP collimator is used. In the case of 360 keV or 300 keV collimator, the output image contrast decreases to 80% or 70% of the input object contrast, respectively. From the physical performance, it is concluded that the photon-deficient lesion is well imaged by the HRP collimator, then the 360 keV, the 300 keV collimator if the statistical fluctuation of count densities can be ignored.

Fig. 6 shows the modified Rollo phantom images with count density of 2.5 kcounts/cm^2, taken apart 10 cm from the surface of collimator (acryl plate with 5 cm thick is inserted between the

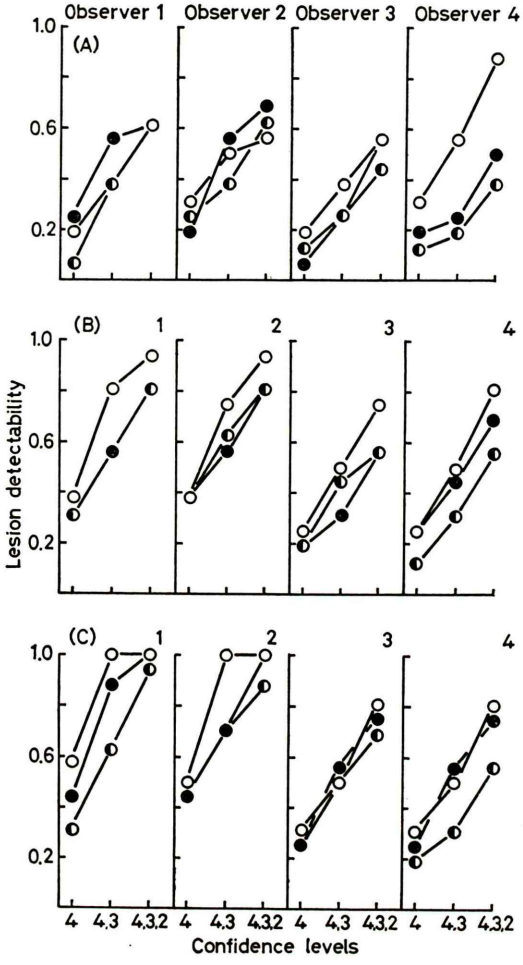

Fig. 8 Lesion detectability at various confidence levels calculated by Eq. 5 on the basis of detection test on the phantom images taken at the surface of colimator. ○: HRP collimator; ●: 360 keV collimator; ◐: 300 keV collimator. (A) count density of 0.5 kcounts/cm²; (B) 1.5 kcounts/cm²; (C) 2.5 kcounts/cm². Lesion detectability, LD, with level of confidences 4,3 is the sum of the LD corresponding to the level of confidence 4 and 3. The LD with level of confidence 4, 3, 2 is the sum of the LD corresponding to level of confidence 4, 3, and 2.

phantom and collimator as a scattering medium), while its observer performance is shown in Fig. 7. Although discrepancies of level of confidence assigned to each lesion were recognized among

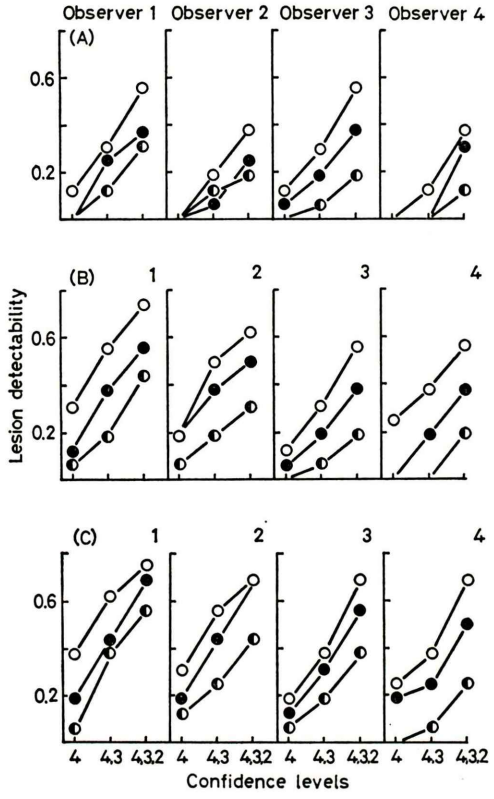

Fig. 9 Lesion detectability at various confidence levels calculated by Eq. 5 on the basis of detection test on the phantom images taken apart 10 cm from the surface of collimator. Symbols, see the notes in Fig. 8.

four observers, it can be seen that detection of lesions decreases with a decrease in lesion size or object contrast. As a measure of observer performance, lesion detectability, LD, expressed as Eq. 5 was tentatively calculated for three levels of confidence ((4)—(2)) and the results were shown in Figs. 8 and 9.

$$\mathrm{LD} = \frac{\text{Sum of detected photon-deficient lesions}}{\text{Number of photon-deficient lesions in phantom } (=16)} \tag{5}$$

As the FWHM in Fig. 2 shows, the difference of system spatial resolution for three parallel hole collimators becomes significant with an increase in the collimator-source distance. The lesion detectability obtained from the images taken at

Table 1 The observer performance measured by the lesion detectability on the modified Rollo phantom

Collimator	FWHM (cm)	Order of lesion detectability											
		Observer 1 Count density			Observer 2 Count density			Observer 3 Count density			Observer 4 Count density		
		0.5	1.5	2.5[3]	0.5	1.5	2.5[3]	0.5	1.5	2.5[3]	0.5	1.5	2.5[3]
HRP	0.67[1]	2	1	1[4]	2	1	1	1	1	2	1	1	2
360 keV	0.75	1	2	2[4]	1	3	2	2	3	1	2	2	1
300 keV	0.94	2	2	3[4]	3	2	3	2	2	2	2	3	3
HRP	1.15[2]	1	1	1	1	1	1	1	1	1	1	1	1
360 keV	1.30	2	2	2	3	2	2	2	2	2	2	2	2
300 keV	1.67	3	3	3	2	3	3	3	3	3	3	3	3

1) FWHM at collimator-source distance of 5 cm in Fig. 2.
2) FWHM at collimator-source distance of 15 cm in Fig. 3.
3) kcounts/cm^2.
4) Among numerical numbers (1, 2, 3), 1 denotes the highest lesion detectability, LD. The LD decreases in a following order: 1>2>3.

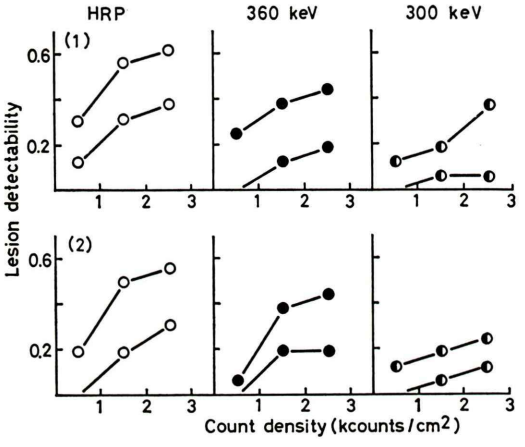

Fig. 10 Lesion detectability as a function of count density. Upper and lower curve of two sets of curves corresponds to the lesion detectability at level of confidence more than 75% and 100%, respectively. (1) result obtained from the observer 1; (2) the observer 2. As the results for the observers 3 and 4 show similar tendency with those for the observers 1 and 2, the latters are shown as representatives.

the surface of collimator does not always reflect that deduced from the physical performance as is shown in Fig. 8. However with an increase in the difference of spatial resolution the physical and observer performance become consistent as is shown in Fig. 9, where the phantom was imaged apart 10 cm from the surface of collimator. These results are summarized in Table 1. In this table, 1, 2, or 3 denotes the order of lesion detectability with three collimators obtained in the level of confidences 4, 3 (corresponds to more than 75% confidence) in Figs. 8 and 9. The lesion detectability as a function of count density is given in Fig. 10, showing clearly the difference among the three collimators. These results lead to conclusion that the observer performance based on the modified Rollo phantom images is useful to evaluate collimator's spatial resolution characteristics.

Discussion

In order to examine the advantage and disadvantage of modified Rollo phantom quantitatively, the lesion detectability, LD, given by Eq. 5 was attempted to calculate as a measure of observer performance. It should be pointed out however that the observer performance in the present work is not so valid as ROC analysis,[4-5] because the observer knows ahead of time that sixteen spherical lesions present in the image regardless of his perception. Therefore it is hard to honestly say whether or not he can see a sphere. Main difference between the present and ROC analysis becomes manifest for lesion with small radius having low object contrast. Namely the lesion corresponding to level of confidence 50% or less, observation may be more or less not only influenced by the fact that he knows previously the presence of lesion but also its surrounding

lesions regularly arranged in the phantom. This perhaps gives higher true positive fraction compared with that obtained in the ROC analysis. On the other hand, as to lesion with larger radius having high object contrast corresponding to level of confidence 75% or more, it may be detected with a similar confidence level even if he can not know ahead of time that it is there. The present analysis, therefore, is inevitably dependent on the assumption that the observers can not be biased by knowing the presence of lesion except large estimation of true positive fraction in their detection tests. If this assumption is permissible, the consistency of observer performance study in Fig. 9 does give our conclusions some credibility.

It is basically possible to determine the contrast efficiency directly by the phantom images without relatively complicated calculation by Eq. 1.[1] As the contrast efficiency is expressing the attenuation of the maximum signal to background ratio Co in the detecting system, the signal count density should be determined over the neighbourhood of the center of sphere. For this purpose, relatively small ROI compared with the lesion sizes in Fig. 1 must be set on the photon-deficient lesions in the image. However it is too difficult to assign the ROI exactly, except the image corresponding to the lesion with large diameter (25.0 mm) having high object contrast (0.71 or 0.50). Thus the contrast efficiency as a function of lesion radius given in Fig. 5 is not determined experimentally. Although it is restricted to special cases being able to determine the image contrast quantitatively, the Rollo phantom is superior to the bar or organ phantom whose data are purely subjective and are not easily quantitated.

Both original and modified Rollo phantoms are designed to simulate the lesions in actual organs (liver, heart, kidney, and thyroid), so that the cell background activity is inevitably different each other. The photographic density of each cell is therefore different. It is too difficult to maintain the image of sixteen photon-deficient lesions within allowable photographic desnity at the same time. Another phantom may be necessary to determine the lesion-detecting ability of imaging system more precisely. For this reason, the phantom consists of four spherical cold (or hot) lesions with different radius within a uniform background activity was made and imaged repeatedly by changing the count density and object contrast. It was found that the signal to noise ratio (S/N) defined by Eq. 6 is a useful measure for recognition of lesions:

$$\frac{S}{N} = \frac{B \times Co \times Ec}{\sqrt{B}} = Co \times \sqrt{B} \times Ec \qquad (6)$$

where B is the background count density (counts/cm^2). If one wishes to detect photon-deficient lesions in the ^{99m}Tc images with a certain level of confidence (practically, 50% or 75% confidence is chosen), the critical S/N value corresponds to such level of confidence in the visual evaluation is required.[6] Thus we can discuss the scintillation camera images from the physical and observer performances points of view.

Conclusions

We discussed the images made with scintillation camera in terms of the physical and observer performances. Among the physical performances the contrast efficiency is relatively complicate to calculate, however it gives the output image contrast for a particular input object contrast. If the image quality can be evaluated by the ease of recognition for the photon-deficient lesions, the contrast efficiency is more effective than the FWHM and MTF.

The lesion detectability, LD, defined by Eq. 5 was used as one of observer performances. The LD was found to reflect approximately the difference of image quality deduced from the physical performances.

A more suitable evaluation method on the image quality which takes into account both physical (expressed as the contrast efficiency) and observer performances is suggested on the basis of the present work.

References

1) Rollo FD: Nuclear medicine physics, instrumentation, and agents. Rollo FD. ed. The C. V. Mosby, Missouri, 1977, p. 387
2) Searle Radiographics: Operation mannual for Pho/Gamma LFOV standard model 6478 or operator's console model 3204
3) Jones JP, Brill AB, Johnston, RE: The validity of an equivalent point source (EPS) assumption used

in quantitative scanning. Phys Med Biol **20**: 455–464, 1975.
4) Goodenough DJ, Rossmann K, Lusted LB: Radiographic Applications of receiver operating characteristic (ROC) curves. Radiology **110**: 89–95, 1974
5) Metz CE: Basic principles of ROC analysis. Sem Nucl Med **8**: 283–298, 1978
6) Shinohara H, Koga Y: Evaluation of scintillation camera by spherical lesion detectability. Radioisotopes **29**: 12–16, 1980